Electron microscopy

Luder, H U ; Amstad-Jossi, M

Abstract: Correlative light (LM) and transmission electron microscopic (TEM) analysis is useful, if ultrastructural details of cells need to be related to functional aspects which can only be examined at the LM level. The first protocol presented here introduces a relatively simple way of obtaining TEM images which, on the one hand, reveal ultrastructural details of individual cells and, on the other hand, are large enough to allow a correlation with light micrographs. The second protocol describes a technique for estimating mineral densities of hard tissues using backscattered electron images obtained with a scanning electron microscope. This technique can be used to analyze the mineralization processes which occur throughout tooth formation.

DOI: https://doi.org/10.1007/978-1-61779-860-3_9

Electron Microscopy

Hans U. Luder and Margrit Amstad-Jossi

Corresponding author: Prof. Dr. Hans Ulrich Luder
University of Zurich
Center of Dental Medicine
Department of Oral Biology
Plattenstrasse 11
CH-8032 Zurich
Switzerland
Phone: +41 44 634 31 40
Fax: +41 44 634 43 06
e-mail: hansulrich.luder@zzm.uzh.ch

Running Head: Electron Microscopy

Summary

Correlative light (LM) and transmission electron microscopic (TEM) analysis is useful, if ultrastructural details of cells need to be related to functional aspects which can only be examined at the LM level. The first protocol presented here introduces a relatively simple way of obtaining TEM images which, on the one hand, reveal ultrastructural details of individual cells and, on the other hand, are large enough to allow a correlation with light micrographs. The second protocol describes a technique for estimating mineral densities of hard tissues using backscattered electron images obtained with a scanning electron microscope (SEM). This can be used to analyze the mineralization processes which occur throughout tooth formation.

Key words: Correlative transmission electron microscopy, Scanning electron microscopy, Calibrated backscattered electron imaging, Hard tissues, Mineral density estimation

1. Introduction

Electron microscopy is a well established technique comprising a wide range of methods for TEM and SEM applications, therefore, numerous guidelines already exist which deal with both basic and advanced techniques ***(1-5)***. The question then is whether ultrastructural investigations related to odontogenesis require any special procedures. Although the protocols described below are applicable also in other fields of research they are dealt with here because they are particularly useful for TEM and SEM investigations of tooth formation.

The first procedure provides a relatively simple way of obtaining correlative LM and TEM data. A common problem faced when examining specimens with the TEM is the fact that its magnification range starts approximately where that of the LM ends. As a result, it can be difficult to identify the area of interest which has already been established at the LM level. This however is important when observing the subtle changes in morphology which, for example, occur in the course of ameloblast and odontoblast differentiation and are associated with alterations in signalling which are usually investigated with the LM. The solution provided by the procedure described below uses a series of TEM micrographs which are taken at relatively high magnifications of large ultrathin sections. These micrographs are then assembled into a composite image which provides an overview of an area which can be easily correlated with conventional LM images and allows the recognition of ultrastructural details of individual cells without digital enlargement (**Fig. 1**). The method does not, however, necessarily yield LM and TEM views of identical cells, as is the case when following some of the techniques described in the guidelines published by Hayat ***(6)***.

The second procedure provides an estimate of the mineral density of hard tissues using micrographs obtained from flat, polished specimens with the backscattered electron (BSE) detector of an SEM (**Fig. 2**). This is useful, because tooth formation is, to a great extent, a calcification process. In particular, the initial mineralization and subsequent maturation of enamel result in mineral gradients which can be analyzed using the described technique. It relies on the almost linear relationship between the intensity of the BSE signal and the mean atomic number of a compound. Hence, if assumptions can be made as to the chemical nature of the constituent parts of a tissue, their concentrations can be derived from the gray level of a BSE micrograph. Various attempts have been made to estimate mineral densities in this way, not only of bone ***(7-13)***, but also of sound and diseased teeth ***(14, 15)***. Unfortunately, the procedures applied have not been described systematically or in detail. The step-by-step guidelines below are an attempt to do that. If the assumptions underlying the calculation are taken into consideration and data are interpreted carefully, the obtained mineral density estimates obtained provide more realistic information than a simple analysis of gray levels

(16), particularly if data are derived from several areas of one specimen and can be analyzed in a comparative way (**Fig. 3B**).

2. Materials

Since the suitability and preparation of materials used for electron microscopic tissue processing, embedding, and sectioning are dealt with comprehensively in earlier work ***(1, 3-5, 17)***, the following list comprises only those solutions, materials, and equipment which we routinely use in our laboratory.

2.1 Specimen Processing

1. Half-strength Karnovsky's fixative: 2% paraformaldehyde, 2.5% glutaraldehyde, 0.025% Ca-chloride, 0.02 M Na-cacodylate (pH 7.2-7.4)
2. Phosphate-buffered fixative: 4% paraformaldehyde, 0.2% glutaraldehyde, 0.1 M phosphate buffer (pH 7.2-7.4)
3. Postfixation: 1.33% Os-tetraoxide, 0.067 M s-collidine
4. Wash-buffer: 0.185 M Na-cacodylate (pH 7.2-7.4)
5. Decalcification: 10% EDTA (Titriplex III; Merck), 0.2% glutaraldehyde

2.2 Embedding

1. Epon: 122 g Epon 812, 79.5 g DDSA, 53.5 g MNA, 3.82 g N,N-benzyldimethylamine
2. Beem capsules: Size 00 with 8 mm inner diameter
3. Technovit 7200 VLC (Heraeus Kulzer)
4. Technovit 7200 embedding molds (Heraeus Kulzer)
5. EXAKT light polymerization unit (EXAKT, Norderstedt, Germany)

2.3 Sectioning

1. Diamond knives (Diatome): histo diamond knife with 6 mm cutting edge or ultra diamond knife with 2.5 mm cutting edge
2. Grids: Parallel bar copper grids coated with a collodion support film (made with 2% collodion in amyl acetate; Electron Microscopy Sciences) with an about 5 nm thick carbon coat

2.4 Staining and Contrasting

1. Toluidine blue: 1% Toluidine blue O, 1% Borax
2. Uranyl acetate: saturated solution in double-distilled water
3. Lead citrate: 0.3% lead citrate in double distilled water

2.5 Grinding and Polishing

1. SEM aluminium stubs 13 mm, 25 mm, or 32 mm in diameter
2. Silicon carbide paper for wet grinding: 180, 1200, and 4000 grit (Struers)
3. Polishing cloth and diamond paste with 3 µm, 1 µm, and 0.5 µm grain sizes
4. EXAKT Grinding System (EXAKT)

2.6 Backscatter Calibration

1. MAC standard #6207 (containing aluminium and carbon; Micro-Analysis Consultants)

2.7 Software

1. Photoshop Version 4 or higher (Adobe)
2. SigmaScan Pro Version 5 (SPSS)
3. Excel (Microsoft)

3. Methods

3.1 Correlative LM and TEM Examination

As fixation, decalcification, dehydration, embedding, sectioning, and staining/contrasting are routine procedures in laboratories equipped for processing TEM specimens, the following list includes only the steps required when a resin block is ready for sectioning. Furthermore, details are described only for the steps which are specific to the technique introduced here.

1. Cut a few survey sections from the resin block containing the entire specimen with a glass or diamond knife and stain them with toluidine blue. If necessary, adjust the plane of sectioning. Identify the area of interest and reduce the block size accordingly.
2. Using a histo diamond knife (or a glass knife), cut some sections of 1-2 µm in thickness and stain them with toluidine blue.
3. Using a histo diamond knife (or an ultra diamond knife, if the block is small enough), cut ultrathin sections of silver-gold interference color (80-100 nm) and collect them on coated grids. Try to place areas intended for TEM examination over gaps between grid bars.
4. Wearing latex gloves, contrast the sections with uranyl acetate and lead citrate.
5. Tranfer a grid to the TEM, turn on the appropriate high tension (we normally use 60 or 80 kV), and select the lowest possible magnification. Having located the area of interest identified in the LM, increase the magnification to the desired value (*see* **Note 1**). It may be advantageous to rotate the grid so as to align the grid bars approximately parallel to the x- or y-axis of the specimen stage.

Capture the micrographs

6. With the image acquisition software of the TEM camera define the background correction (sometimes also referred to as shading) and determine the optimal exposure settings at the selected magnification. Then identify one corner of the intended composite image and, starting from this point, collect contiguous rows and columns of micrographs by displacing the specimen stage only along either the x- or y-axis. Make sure that individual micrographs overlap by about 10%. Use constant exposure settings as determined at the start of capturing throughout the image acquisition.

Assemble the micrographs in Photoshop

7. Based on a rough estimate of the final size of the composite image, create a new document with a canvas size sufficient to accommodate the constituent micrographs (*see* **Note 2**).
8. Open a series of 10-12 constituent micrographs (*see* **Note 3**). Depending on their original resolution as well as on the number of collected images, reduce the size of the constituent micrographs (ex. to about 600-700 x 600-700 pixels) in order to avoid excess amounts of data for the composite image.
9. Select the first micrograph and adjust levels to range from about 5 (almost black) to 250 (almost white). Based on visual judgement, the brightness should be medium. With the Move tool, drag the micrograph to the appropriate corner of the canvas of the composite image, thereby creating a new layer. Label this layer for easy later identification.
10. Select the subsequent micrograph and drag it to a new layer of the composite image. Label this layer as well and, using the Zoom tool, zoom in to see only the two micrographs which have to be superimposed. In the Layer menu, create a new adjustment layer for level adjustment, make sure to activate Create Clipping Mask in the pop-up window (*see* **Note 4**), and adjust levels. If necessary, adjust also brightness and contrast in the same way, until the visual appearance of both micrographs correspond. Optionally, merge down adjustment layers to image layer (*see* **Note 5**).
11. Select the image layer and, using the glider in the Layers panel menu, reduce the opacity of the image to 50-60%, select the Move tool and superimpose conspicuous structures in the overlapping portion of the two micrographs. Coarse movements are made with the mouse, fine adjustments with the arrow keys. Restore the opacity of the image layer.

12. In the Layer menu create a layer mask. With the Brush tool and black selected as foreground color, remove the margin of the micrograph which is often slightly darker and irritating (*see* **Note 6**). If an irregular margin is thus created, the transition from one image to the next becomes less conspicuous.
13. Save the composite image, preserving all layers (*see* **Note 7**).
14. Repeat steps 10-13 for all remaining micrographs.
15. Crop the final image to the desired size and (optionally) flatten it to one level to reduce the amount of required storage space required.

3.2 Mineral Density Estimation

Carry out all procedures involving fixatives, solvents, and embedding media in a fume hood and wear latex gloves.

1. Fix specimens in half-strength Karnovsky's fixative or phosphate-buffered fixative (*see* **Note 8**), thereafter rinse them thoroughly in wash buffer.
2. Depending on the intended plane of sectioning, create a flat specimen surface for embedding with a razor blade, diamond saw, or file.
3. Dehydrate the specimens in ascending grades of ethanol (one half-day, each, in ethanol concentrations from 50% to 95%, a full day in 100% ethanol).
4. Infiltrate with Technovit 7200 VLC (1 day in a 2+1-mixture of ethanol and Technovit, 2 days, each, in 1+1- and 1+2-mixtures, 1 week in 100% Technovit under vacuum of about 300 mbar). Avoid premature polymerization of the resin due to daylight irradiation by using brown glass vials and/or wrapping the vials with aluminium foil.
5. Embed specimens on the flat surface in Technovit 7200 VLC using molds of appropriate size. Avoid introducing air bubbles and place molds in vacuum for 5-10 minutes before polymerization.
6. Place molds in a cold water bath which is preferably cooled with running water, cover them with a thin Plexiglas plate and polymerize the Technovit with white light for 2 hours followed by blue light for 2 hours (*see* **Note 9**).
7. Remove blocks from embedding molds (*see* **Note 10**) and glue them onto SEM aluminium stubs, taking care that the flat specimen surface is as parallel as possible to the stub surface.
8. Expose the area of interest of the specimen by wet grinding the block surface with silicon carbide papers of decreasing grit size. Visual controls with a stereomicroscope may be necessary to determine, whether enough resin has been removed. When this is achieved, the block is polished with a polishing cloth and diamond pastes of grain sizes 3 µm, 1 µm, and finally 0.5 µm (*see* **Note 11**).
9. Let the blocks dry at room temperature for several days. Then coat the polished surfaces with a 10-15 nm thick layer of carbon.
10. Place a block together with aluminium and carbon standard samples in the SEM chamber (*see* **Note 12**). Select BSE mode and turn the high tension (20 kV) on. Let the filament stabilize for at least 15-30 minutes (*see* **Note 13**).
11. Select a working distance of 20-25 mm and leave it constant. Focus the standards and specimen only using the Z-drive of the microscope stage (*see* **Note 14**). Adjust gain and contrast of the signal so as to obtain a gray level of about 200-210 for aluminium and of about 5-10 for carbon (*see* **Note 15**).
12. Leaving the settings for gain and contrast as well as the working distance fixed, capture the necessary micrographs of the specimen (**Fig. 1A-E**) and then one micrograph, each, of the aluminium and carbon standard.
13. Open micrographs of the specimen in SigmaScan Pro. If deemed necessary, calibrate distances to change the scale from pixels to mm or µm. Determine gray level values either as averages within an area of interest or at individual dots along a line. In the same way,

record mean gray level values from the micrographs of the aluminium and carbon standard. For this purpose, select Trace Measurements Mode and the following parameters from the Measurements Settings: Measurements Average Intensity or Line Intensity, the Column of the worksheet, where data are to be collected, an Overlay for the drawing, and Continuous (Streaming) Measurements for Trace mode (if Line Intensity has been selected, the Line Width in pixels is also defined here). Then outline an area or draw a line using the left mouse key, terminate drawing with a right mouse click. This automatically creates a worksheet containing the data in the selected column. Save this worksheet as an Excel file.

14. Make the necessary assumptions regarding the approximate chemical composition of the compound hard tissue (*see* **Note 16**) and calculate the respective mean atomic numbers (MAN) and mean backscatter coefficients (MBSC; *see* **Note 17**). We routinely use Müller's and Lloyd's formula for MAN and Castaing's formula for MBSC ***(18)*** (indicated as entered in an Excel formula):
    MAN = SUM(c_i*Z_i) for i = 1 to n constituent elements, where
    c_i = weight fraction of element i with atomic number Z_i
    $MBSC$ = SUM(c_i*BSC_i) for i = 1 to n constituent elements, where
    c_i = weight fraction of element i with backscatter coefficient BSC_i = 2^(-9/SQRT(Z_i))
    Table 3.1 lists MANs and MBSCs useful for mineral density estimation.
15. Open the worksheet containing the raw gray level data in Excel and derive the MBSC of the compound tissue ($MBSC_{Tissue}$). Then calculate the mineral density estimates (MDE; in weight%; *see* **Note 18**) as follows (indicated as entered in an Excel formula):
    $MBSC_{Tissue} = (BSC_{Al}*(I_{Tissue} - I_C) + BSC_C*(I_{Al} - I_{Tissue}))/(I_{Al} - I_C)$
    where BSC_{Al} and BSC_C = BSCs of aluminium and carbon (Table 3.1)
    I_{Tissue} = graylevel value obtained from compound hard tissue (0-255)
    I_{Al} and I_C = graylevel values obtained from the aluminium and carbon standard

    If water is disregarded
    $MDE = (MBSC_{Tissue} - MBSC_{Matrix})/(MBSC_{Mineral} - MBSC_{Matrix})$
    where $MBSC_{Mineral}$ and $MBSC_{Matrix}$ = MBSCs of mineral phase and organic matrix (Table 3.1)

    If water is assumed to be present at a proportion of e.g. 1 part matrix : 4 parts water
    $MDE = (MBSC_{Tissue} - MBSC_{Matrix})/5 - 4*MBSC_{Water}/5)/(MBSC_{Mineral} - MBSC_{Matrix}/5 - 4*MBSC_{Water}/5)$
    where $MBSC_{Water}$ = MBSC of water (Table 3.1)

4. Notes

1. In order to recognize ultrastructural details of individual cells, a minimum magnification of about 1900-2000x is required. Depending on the size of the area of interest, this may necessitate more than 100 micrographs.
2. The estimate of canvas size is not critical, as it can be adjusted at any time during assembling.
3. The advantage of opening several micrographs at a time is twofold. First, some of the subsequent steps can be carried out using batch processing and second, the original appearance of the images can readily be restored, if some of the adjustments made turn out to have been inappropriate.
4. If a clipping mask is not created, all adjustments made in an adjustment layer affect all images deeper down in the layer list.
5. Merging down adjustment layers reduces the length of the layer list which can become extensive and rather obscured, if large numbers of micrographs are assembled. The

advantage of keeping the adjustment layers is that individual constituent images can be further modified (or restored to the original appearance) at any time.

6. When white is selected as foreground color, all changes made with the Brush tool can be reversed.
7. For easy identification, we use the Photoshop format (.psd) for the compound image including all layers and the TIFF format (.tif) for the flattened image.
8. The choice of fixatives is uncritical. Depending on the size of the specimens, the duration of fixation can vary from 2 hours to several days at room temperature or 4°C.
9. A convenient way of polymerization is provided by the EXAKT light polymerization unit with integrated cooling system.
10. Polymerization of Technovit 7200 VLC is impaired by oxygen from the air. Therefore, the top surface of the polymerized blocks is often rubber-like. When the blocks are stored at room temperature for 1-2 days and unpolymerized monomer is allowed to evaporate, the layer of soft resin can easily be scraped or ground away to produce a hard, rough surface for gluing.
11. In order to keep the block surface parallel to the stub, we grind blocks using the EXAKT grinding system. For this purpose, stubs are fixed in a custom-made holder which can be placed in the specimen holder of the machine like a microscope slide. Polishing is done by hand.
12. Instead of using a commercial product, standards can easily be prepared using small pieces of pure aluminium wire and graphite which are embedded in Technovit 7200 VLC and processed exactly as the specimen blocks.
13. According to our experience, stabilization of the filament is one of the most critical factors for obtaining reproducible gray levels of the BSE signal. This is the reason, why we use embedded rather than hydrated specimens in a low vacuum environment (environmental SEM conditions), in which specimens dry out quickly, making the results of the quantitative analysis unpredictable.
14. The working distance is also a very important factor, because even small variations significantly affect the BSE signal intensity.
15. Modern digital microscopes usually offer the possibility to select an intensity histogram.
16. While it is clear that estimation of biological mineral densities has to take into account at least a mineral phase and the organic matrix, the question is whether to also consider water (which is even denser than organic matrix). When dehydrated and embedded material is analyzed, disregarding water may be reasonable. If it is to be considered, a further question is whether it is associated mainly with the organic matrix and/or in a certain fixed proportion, for instance the proportion found in normal, fully mineralized tissues. As shown in **Fig. 3A**, this assumption markedly affects the resulting estimates of mineral density, particularly when the contents of organic matrix are relatively high.
17. As revealed by Fig. 3A, using MANs instead of MBSCs has little impact on the resulting mineral density estimates. Moreover, there is no consensus as to the correct way of calculating MANs and MBSCs, and values obtained with the various methods differ considerably ***(18)***.
18. We do not calculate volume fractions, because this would require still another assumption as to the specific weight of the tissue components.

Acknowledgement

The authors thank Jacqueline Hofmann-Lobsiger and Steven Reese for the skilful preparation of the specimens used for the illustrations of this work.

References

1. Pease DC (1964) Histological techniques for electron microscopy, 2nd edn. Academic Press, New York.
2. Hayat MA (1970-1978) Principles and techniques of electron microscopy: biological applications, vol 1-9. Van Nostrand Reinhold Company, New York.
3. Glauert AM (ed) (1972-1992) Practical methods in electron microscopy, vol 1-14. North Holland, Elsevier, Amsterdam.
4. Koehler JK (ed) (1973) Advanced techniques in biological electron microscopy. Springer-Verlag, Berlin, Heidelberg.
5. Hayat MA (2000) Principles and techniques of electron microscopy: biological applications. Cambridge University Press, Cambridge (UK).
6. Hayat MA (ed) (1987) Correlative microscopy in biology: instrumentation and methods. Academic Press, Orlando (FL).
7. Sutton-Smith P, Beard H, Fazzalari N (2008) Quantitative backscattered electron imaging of bone in proximal femur fragility fracture and medical illness. J Microsc 229:60-66.
8. Roschger P et al (1995) A new scanning electron microscopy approach to the quantification of bone mineral distribution: Backscattered electron image grey-levels correlated to calcium Kα-line intensities. Scanning Microsc 9:75-88.
9. Bloebaum RD et al (1997) Determining mineral content variations in bone using backscattered electron imaging. Bone 20:485-490.
10. Skedros JG et al (1993) The meaning of graylevels in backscattered electron images of bone. J Biomed Mater Res 27:47-56.
11. Skedros JG et al (1993) Influence of mineral content and composition on graylevels in backscattered electron images of bone. J Biomed Mater Res 27:57-64.
12. Vajda EG, Skedros JG, Bloebaum RD (1995) Consistency in calibrated backscattered electron images of calcified tissues and minerals analyzed in multiple imaging sessions. Scanning Microsc 9:741-755.
13. Boyde A et al (1992) Applications of mineral quantitation of bone by histogram analysis of backscattered electron images. In: Slavkin H, Price P (eds) Chemistry and biology of mineralized tissues. Elsevier Science Publishers B.V., Amsterdam, p 47.
14. Angker L et al (2004) Correlating the mechanical properties to the mineral content of carious dentine - a comparative study using an ultra-micro indentation system (UMIS) and SEM-BSE signals. Arch Oral Biol 49:369-378.
15. Angker L et al (2004) Quantitative analysis of the mineral content of sound and carious primary dentine using BSE imaging. Arch Oral Biol 49:99-107.
16. Mahoney EK et al (2004) Mechanical properties and microstructure of hypomineralised enamel of permanent teeth. Biomaterials 25:5091-5100.
17. Hayat MA (1981) Fixation for electron microscopy. Academic Press, New York.
18. Howell PGT, Davy KMW, Boyde A (1998) Mean atomic number and backscattered electron coefficient calculations for some materials with low mean atomic number. Scanning 20:35-40.
19. Harada H, Ohshima H (2004) New perspectives on tooth development and the dental stem cell niche. Arch Histol Cytol 67:1-11.
20. Driessens FCM, Verbeek RMH (1990) Biominerals. CRC Press, Boca Raton (FL), p 131.

Table 3.1. Mean atomic numbers (MAN) and mean backscatter coefficients (MBSC) useful for mineral density estimation of hard tissues.

Compound	MAN	MBSC
Tooth mineral $Ca_9[(PO_4)_{4.5}(CO_3)_{1.5}]OH_{1.5}$ ***(20)***	13.871	0.179
Organic matrix ***(13)***	6.4	0.085
Water	7.217	0.098
Aluminium	13.0	0.177
Carbon	6.0	0.078

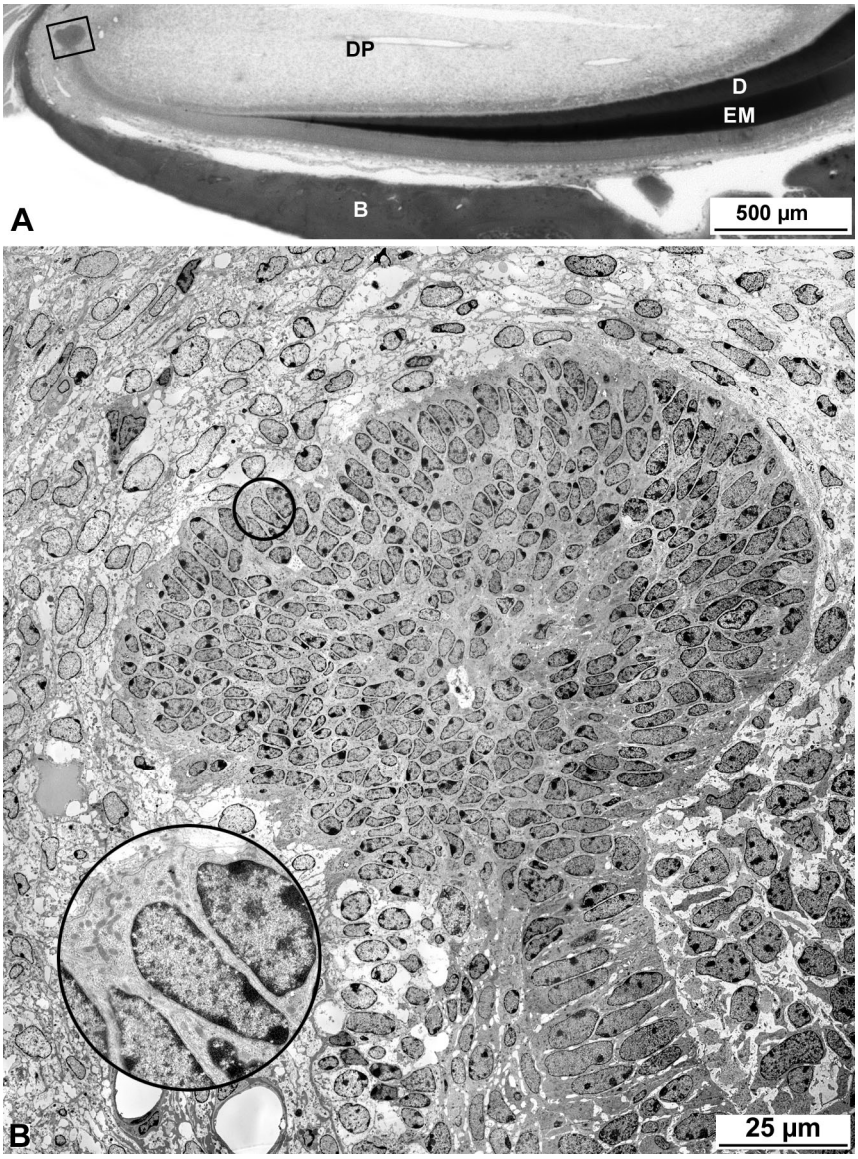

Fig. 1. Light (**A**) and transmission electron (**B**) micrographs of the cervical loop of a lower incisor from a 3 week-old mouse. The structure marked by the rectangle in **A**, resembling the head-like structure described by Harada and Ohshima ***(19)***, is displayed in **B**. The inset in **B** is a closer view, obtained without any digital enlargement, of the detail marked by the circle. B = bone, D = dentin, DP = dental papilla, EM = enamel matrix. Original magnifications (**A**) 20x, (**B**) 1950x.

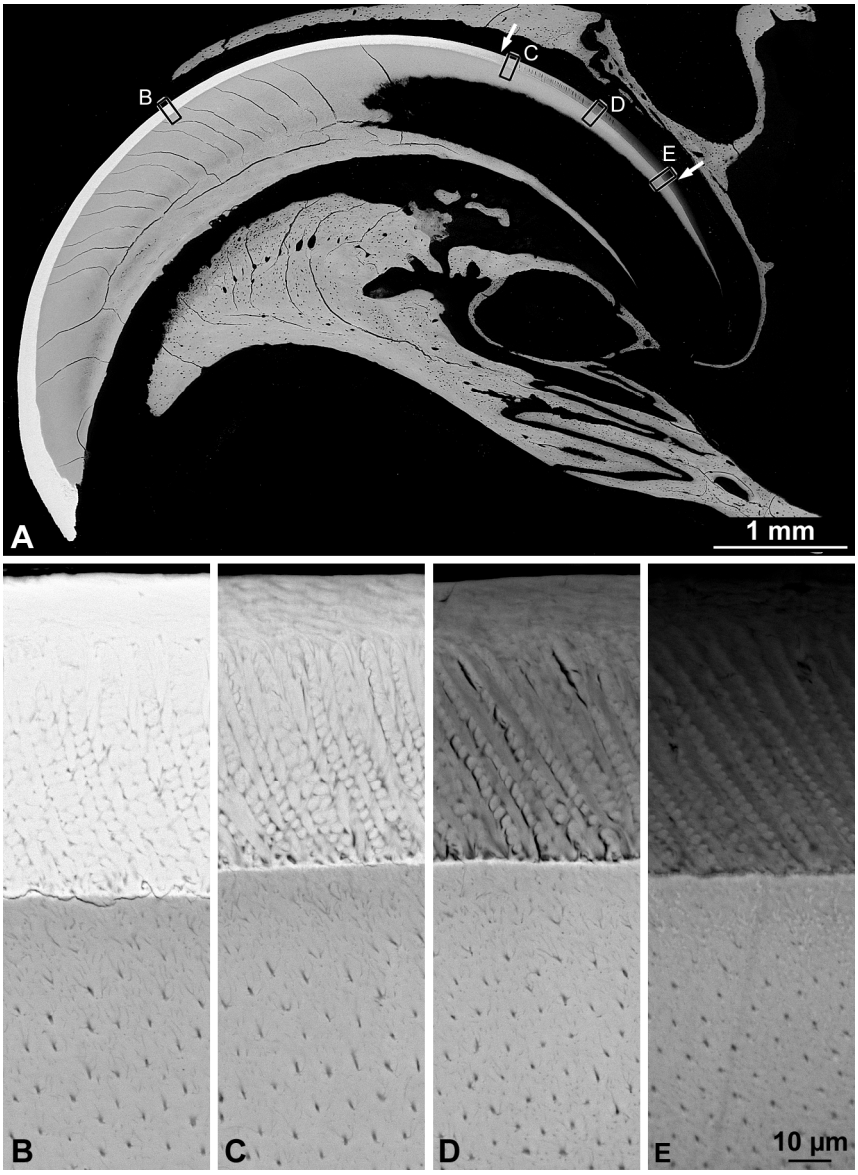

Fig. 2. Calibrated backscatter electron micrographs of an upper incisor from a 3 week-old mouse, which were used for estimating the mineral densities (MDE) represented graphically in **Fig. 3**. (**A**) Overview; the two arrows delineate the zone of enamel maturation which was analyzed as indicated in **Fig. 3A**; the rectangles labelled B, C, D, and E mark the location of the details shown in **B-E**. (**B-E**) Details of the enamel and peripheral dentin after eruption (**B**) as well as at the end (**C**), in the middle (**D**), and at the beginning (**E**) of the zone of enamel maturation. MDEs across the enamel in these areas are graphically displayed in **Fig. 3B**. Original magnifications (**A**) 100x, (**B-E**) 2000x.

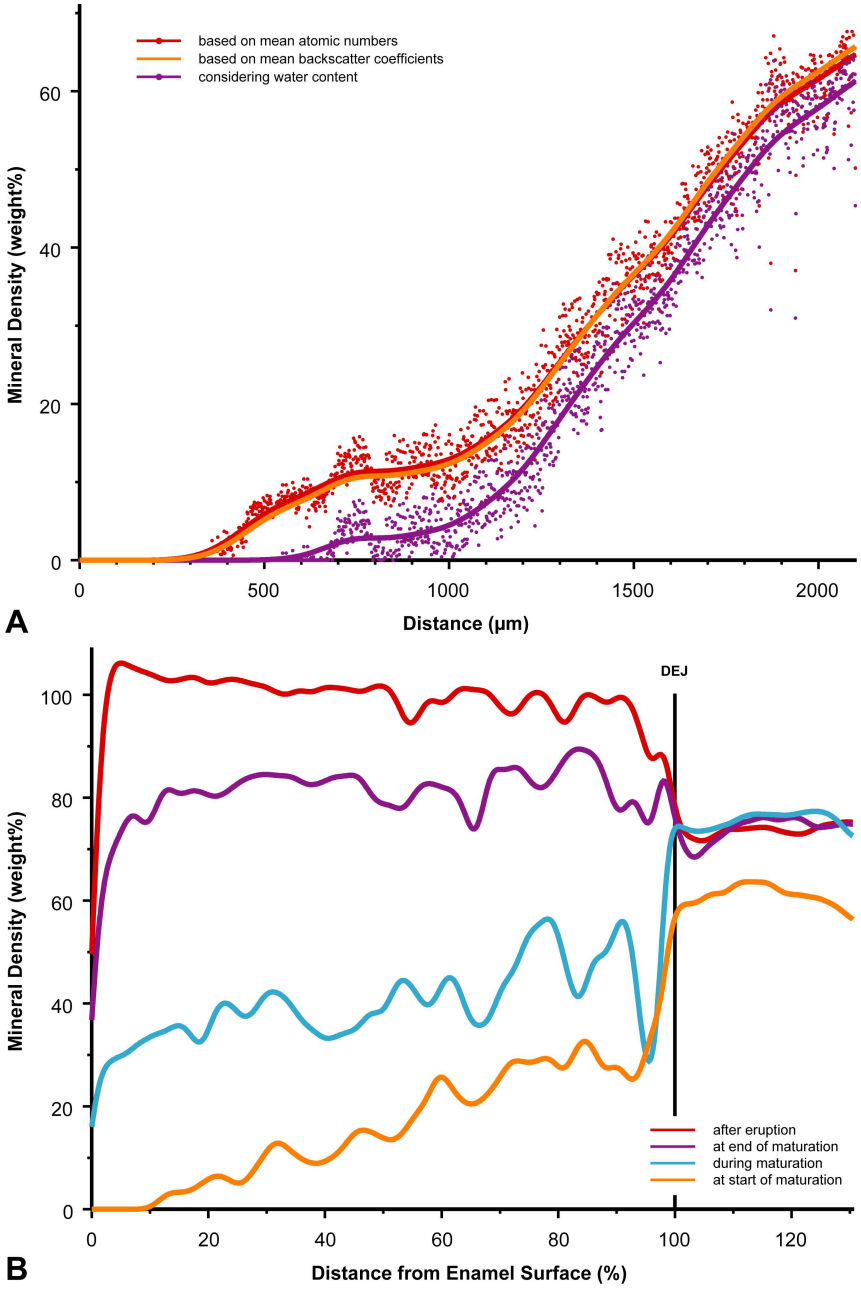

Fig. 3. Graphical representations of mineral density estimates (MDE) made on the micrographs shown in **Fig. 2**. (**A**) MDE obtained from a 5 pixel-wide line in the middle of the enamel layer from the beginning to the end of enamel maturation indicated by the arrows in **Fig. 2A**. MDEs plotted as solid line and dots were derived on the basis of mean atomic numbers, MDEs represented as irregularly dotted line (close by the solid line) were obtained on the basis of mean backscatter coefficients, and MDEs plotted as open circles and the regularly dotted line were calculated under the assumption that water was present in a proportion of 4 parts water per 1 part organic matrix. (**B**) MDEs obtained from 5 pixel-wide lines across the areas of enamel and peripheral dentin shown in **Fig. 2B-E**. It was assumed that no water was present either in enamel or dentin. The distance from the surface is indicated as percent of the total enamel thickness (0-100%) and of the total dentin thickness (100-200%); as a consequence, the dentin-enamel junction (DEJ) is located at a distance of 100% from the surface.